Weighted shortest path in equilateral triangular meshes*

Prosenjit Bose† Guillermo Esteban‡ § Anil Maheshwari¶

Abstract

Let $\mathcal{T}$ be a tessellation composed of equilateral triangular regions, in which each region has an associated positive weight. We present two approximation algorithms for solving the Weighted Region Problem. Our algorithms are based on the method of discretizing the space by placing points on the cells of the tessellation and using Dijkstra's algorithm for computing the weighted shortest path in the geometric graph obtained by such a discretization. For a given parameter $\varepsilon \in [0, 1]$, the weight of our paths are $\left(1 + \frac{14(4\sqrt{2}\sqrt{\sqrt{6\varepsilon}+8}-\sqrt{6\varepsilon}-8)-16(7+\varepsilon)}{(-4\sqrt{2}\sqrt{\sqrt{6\varepsilon}+8}+\sqrt{6\varepsilon}+8)(7-\varepsilon)}\right) \leq 1 + 0.39\varepsilon$, and $1 + \varepsilon$ (using fewer points) times the cost of the actual shortest path.

1 Introduction

In this paper, we study optimal obstacle-avoiding paths from a starting point s to an ending point t in the 2-dimensional plane. Shortest path problems are among the most studied problems in computational geometry. These problems have applications in several areas such as robotics [16], video-games [11, 17], and geographical information systems (GIS) [7], among others.

Mitchell and Papadimitriou [13, 12] examined a generalization of the shortest path problem, called the Weighted Region Problem (WRP). They allowed the two-dimensional space to be subdivided into regions, each of which has a (non-negative) weight associated to it, representing the cost per unit distance of traveling in that region. They provided an approximating algorithm which computes a $(1 + \varepsilon)$-approximation path in $O(n^8 \log \frac{nNW}{w\varepsilon})$ time, where N is the maximum integer coordinate of any vertex of the subdivision, W (respectively, w) is the maximum finite (respectively, minimum non-zero) integer weight assigned to faces of the subdivision.

Motivated by this result, several authors proposed algorithms for computing approximated paths, reducing the running time and producing geometric problem instances with fewer "bad" configurations (e.g., the Delaunay triangulation is used to maximize the minimum angle).

The most common scheme followed in the literature is to position Steiner points, and then build a graph by connecting pairs of Steiner points. An approximate solution is constructed by finding a shortest path in this graph, by using well-known combinatorial algorithms (e.g., Dijkstra's algorithm).

Aleksandrov et al. [3, 4] proposed placing Steiner points on edges of an appropriate mesh, and then, interconnecting the Steiner points within each face. Since an infinite number of Steiner points would be required for the approximation, they constructed a star shaped polygon around each vertex of the mesh; ensuring that Steiner points are placed outside these regions. They also deal with the problem of large sized graphs. By deriving geometric properties of Snell's law of refraction for a discrete domain, they reduced the search space. They employed a pruned Dijskstra's algorithm where the execution is restricted to a sparse set of potential edges, given that the preceding edge on a path is known. Employing all these steps together and using geometric spanners they obtained a $(1 + \varepsilon)$-approximation path.

Reif and Sun [18] used the same discretization approach as in [4]. They employed an algorithm called BUSHWHACK to compute an optimal path in the discrete graph by dynamically adding edges.

In addition, Aleksandrov et al. [5] used a similar approach as in [4], but placing, for the first time, the Steiner points on the bisectors of the angles, and not on the face boundaries. However, this complicates computation of the discrete path because now the edges join Steiner points that belong to neighboring faces.

See Table 1 for the time complexity of the approximation algorithms designed following these schemes.

Recently, it has been shown that the WRP cannot be solved exactly within the Algebraic Computation Model over the Rational Numbers (ACM$\mathbb{Q}$) [6], i.e., a solution to an instance of the WRP cannot be expressed as a closed formula in ACM$\mathbb{Q}$. This emphasizes the need for high-quality approximate paths instead of optimal paths. So, in practice, the geometric space is discretized

*Partially supported by NSERC, project PID2019-104129GB-I00/MCIN/AEI/ 10.13039/501100011033 of the Spanish Ministry of Science and Innovation, and H2020-MSCA-RISE project 734922 - CONNECT.

†School of Computer Science, Carleton University, Canada, jit@scs.carleton.ca

‡Departamento de Física y Matemáticas, Universidad de Alcalá, Spain,

§School of Computer Science, Carleton University, Canada g.esteban@uah.es

¶School of Computer Science, Carleton University, Canada, anil@scs.carleton.ca

Time complexity	Reference
$O(n^8 \log \frac{nNW}{w\varepsilon})$	[13]
$O(N^4 \log \left(\frac{NW}{w\varepsilon}\right) \frac{n}{\varepsilon^2} \log \frac{nN}{\varepsilon})$	[3]
$O(N^2 \log \left(\frac{NW}{w}\right) \frac{n}{\varepsilon} \log \frac{1}{\varepsilon} (\frac{1}{\sqrt{\varepsilon}} + \log n))$	[4]
$O(N^2 \log \left(\frac{NW}{w}\right) \frac{n}{\varepsilon} \log \frac{n}{\varepsilon} \log \frac{1}{\varepsilon})$	[18]
$O(N^2 \log \left(\frac{NW}{w}\right) \frac{n}{\sqrt{\varepsilon}} \log \frac{n}{\varepsilon} \log \frac{1}{\varepsilon})$	[5]

Table 1: ε-approximation algorithms for the Weighted Region Problem.

using grids. The concept of grid is essential and heavily used in digital elevation models (DEMs) [2, 10] and in video games [8]. Because of their symmetry and natural neighborhood structure, regular triangle meshes are preferred over square and hexagonal.

Although it is the most complex among the three regular tessellations (it has the largest number of vertices), it has various advantages in applications, e.g., the distance between the vertices of adjacent cells is always the same, which simplifies distance calculations. Triangles can represent complex shapes, and they can include hexagonal grids. Although they are built with triangles in two different orientations, each pixel has 12 neighbors sharing at least a corner, which gives a valid alternative for applications in image processing. Recently, various image processing algorithms have been defined and implemented for the triangular grid, such as discrete tomography [14, 15], thinning [9], and mathematical morphology [1].

1.1 Our results

In this paper, we present algorithms for computing approximate shortest paths between two vertices s and t on a triangular tessellation. We work with the particular case in which every cell of the mesh is an equilateral triangle. In addition, each cell has a positive real weight associated to it.

Our results are based on a previous work of Aleksandrov et al. [5]. With a finer analysis, we improve the results in two different ways:

1. If we use the same number of Steiner points as in [5], we prove that the approximation factor is minimized when placing the Steiner points on the edges of the cells. In addition, we provide an upper bound on the quality of the approximation path with respect to the actual shortest path. Our result gives an approximation factor which is at least $\frac{5(1+\varepsilon)(7-\varepsilon)}{7(5+\varepsilon)} \geq 1 + 0.428\varepsilon$ times better than the previous result.

2. If we decide to maintain the approximation factor in each of the cells, we provide a discretization using fewer Steiner points than in [5]. We increase the distance between Steiner points in each segment by about a factor of $\frac{7-\sqrt{\varepsilon}}{40} \approx 0.175 - 0.025\sqrt{\varepsilon}$, which decreases the running time of the algorithm to determine the approximation path.

To solve these problems, we use the traditional technique of partitioning the continuous 2D space into a discrete space by designing an appropriate graph. Differently from the previous work of Aleksandrov et al. [5], the discretization is done by placing Steiner points along a segment from each vertex of the mesh inclined by α radians. Then, we minimize the number of Steiner points to be added by optimization over the angle $\alpha \in [0, \frac{\pi}{3}]$. All these improvements were obtained by taking into account trigonometric properties from the points of entry of the paths into the cells and carrying out a thorough analysis when optimizing the results.

The paper is organized as follows: we start Section 2 by introducing the definitions that are needed for the forthcoming calculations. We also provide Lemma 2, where two properties about the entry and leaving points of the shortest path are calculated. Then, in Section 2.1, with the same number of Steiner points proposed by Aleksandrov et al. [5] we improve their results on the approximation factor of the whole path. Similarly, in Section 2.2, we fix the approximation factor of $1 + \frac{\varepsilon}{2}$ for each segment joining two points on the edges of a cell, and we optimize the number of Steiner points to be placed in each triangular cell. Finally, in Section 3 we compare the results that we obtain with the previous results from [5].

2 Equilateral triangle mesh

Let $\mathcal{T}$ be a triangular tessellation in the 2-dimensional space. We will suppose that $\mathcal{T}$ is a connected union of a finite number of equilateral triangles, denoted by $T_1, \ldots, T_n$. Two triangles of the set can share a vertex, an edge, or not being adjacent. Each face T_i, $i \in \{1, \ldots, n\}$, of the tessellation has a positive weight ω_i associated to it. This weight represents the cost of traveling through a face per unit of Euclidean distance.

Any continuous (rectifiable) curve lying in $\mathcal{T}$ is called a path. Every path in $\mathcal{T}$ consists of a sequence of segments, whose endpoints are on the edges of $\mathcal{T}$. Each of these segments is of one of the following two types:

- face-crossing: the endpoints belong to adjacent edges;
- edge-using: the endpoints belong to the same edge of a face.

The cost of a path π is given by $\|\pi\| = \sum_{i=1}^{n} \omega_i \|\pi_i\|$, where $\|\pi_i\|$ denotes the Euclidean length of the intersection between π and a triangle T_i. In case π_i is an edge-using segment, then the cost of traveling along that

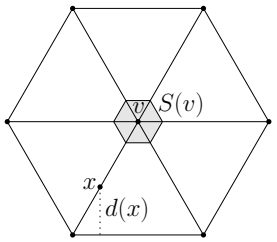

Figure 1: $d(x)$ is the length of the dotted segment. The vertex vicinity of v is depicted in gray.

edge is the minimum of the weights of the triangles incident to the edge. Given two distinct points s and t in $\mathcal{T}$, a shortest path $\pi(s,t)$ is a path that minimizes the weighted distance between s and t. Without loss of generality, we may assume that s and t are vertices of the tessellation.

A path $\pi(s,t)$ is represented by a sequence of points $s = a_0, \ldots, a_\ell = t$ lying on the edges. The points a_i, $i \in \{1, \ldots, \ell - 1\}$, that are not vertices of the tessellation are called bending points of the path.

Following notation from [5], the function $d(x)$ is defined as the minimum Euclidean distance from a point x on a side of a triangle to the boundary of the union of the faces containing x, see Figure 1.

For each vertex v of the tessellation $\mathcal{T}$, let $\omega_{max}(v)$ and $\omega_{min}(v)$ be, respectively, the maximum (finite) weight and the minimum weight of the faces adjacent to v. Let $r(v)$ be the weighted radius of the vertex v defined as follows:

$$r(v) = \frac{\omega_{min}}{7\omega_{max}} d(v)$$

Then, for each face adjacent to v, an equilateral triangle with side length $\varepsilon r(v)$ is defined. Around v, a regular hexagon $S(v)$, called the vertex-vicinity of v, is obtained, see Figure 1. Let e_1 be the edge of T_j that is encountered first when traversing the edges of T_j from v in counterclockwise order. We also define $\ell_v(j,\alpha)$ as the segment in T_j from v inclined by α radians with respect to e_1, see Figure 2.

Definition 1 *Let T_j be an equilateral triangle of the tessellation $\mathcal{T}$, and let v be a vertex of T_j. We define a set of Steiner points $p_0, p_1, \ldots, p_k$ on $\ell_v(j,\alpha)$ by:*

$$|p_{i-1}p_i| = a(\varepsilon)\sin\alpha |vp_{i-1}|, \text{ for } i \in \{1, \ldots, k\}, \quad (1)$$

where $a : (0,1] \to \mathbb{R}$, p_0 is the intersection point between $\ell_v(j,\alpha)$ and the boundary of $S(v)$, and k is the largest integer such that $|vp_k| \leq |\ell_v(j,\alpha)|$.

Lemma 2 *Let e_1, e_2 be two edges adjacent to v in T_j, and let x_1, x_2 be two points in e_1 and e_2, respectively. Let p' be the intersection point between $|x_1x_2|$ and $\ell_v(j,\alpha)$. Let p be the closest Steiner point to p'.*

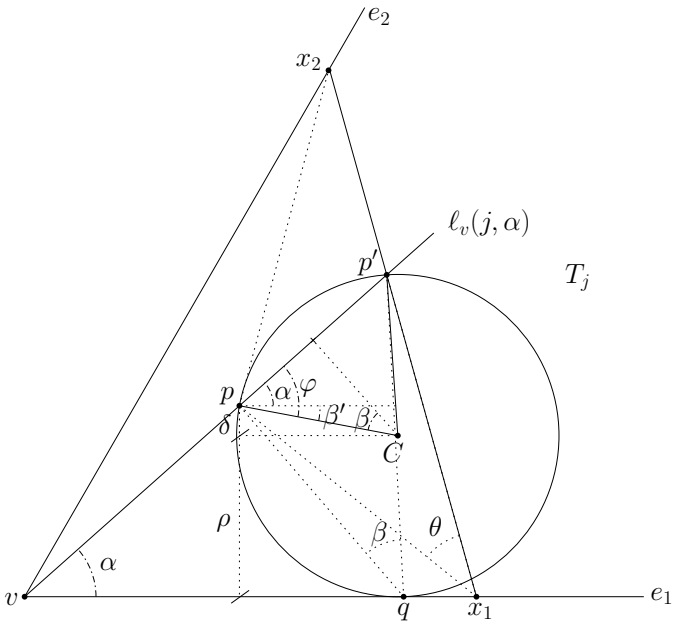

Figure 2: Illustration of Lemma 2.

- *Let θ be the angle $\angle px_1p'$, then*

$$\tan\frac{\theta}{2} \leq \frac{2\sqrt{2}\sqrt{a\sin\alpha + 2} - a\sin\alpha - 4}{a(\cos\alpha - 1)}. \quad (2)$$

- *Let $A = \frac{2\sqrt{2}\sqrt{a\sin\alpha+2}-a\sin\alpha-4}{a(\cos\alpha-1)}$ and $B = \frac{2\sqrt{2}\sqrt{a\sin(\frac{\pi}{3}-\alpha)+2}-a\sin(\frac{\pi}{3}-\alpha)-4}{a(\cos(\frac{\pi}{3}-\alpha)-1)}$, then*

$$|x_1p| + |px_2| \leq \left(1 + \frac{AB}{1-AB}\right)|x_1x_2|. \quad (3)$$

Proof. Let p' belong to the segment $[p_i, p_{i+1}]$. We want to calculate an upper bound on the value of the angle θ, for any x_1 and x_2. It is well known, that θ is maximum when the circle through p, p' and x_1 is tangent to e_1. So, let q be this point of tangency, and let C be the center of the circle. Then, an upper bound on the angle θ is given by the angle $\beta = \angle pqp'$, i.e., $\theta \leq \beta$. Let ρ be the radius of the circle through pqp'. Let $\rho + \delta$ be the distance from p to e_1, see Figure 2. We define the angle $\angle p'pC$ as φ. So, considering the triangle formed by p, C and the midpoint of the segment $\overline{pp'}$, we have that $\pi = \frac{\pi}{2} + \beta + \varphi \Rightarrow \varphi = \frac{\pi}{2} - \beta$. We also define the angle β' as $\beta' = \varphi - \alpha = \frac{\pi}{2} - \beta - \alpha$. Hence,

$$\begin{cases} \sin\beta' = \frac{\delta}{\rho} \Rightarrow \delta = \rho\sin(\frac{\pi}{2} - \beta - \alpha) \\ \sin\alpha = \frac{\rho+\delta}{|vp|} = \frac{\rho(1+\sin(\frac{\pi}{2}-\beta-\alpha))}{|vp|}. \end{cases}$$

Note that the angle β is maximum when p' is the midpoint of the segment $\overline{p_ip_{i+1}}$. Thus, if $p = p_i$, and using equation (1) with the triangle $\triangle qp_ip'$, we get that

$$\begin{aligned}
\sin\beta &= \frac{\frac{|p_ip_{i+1}|}{2}}{2\rho} = \frac{\frac{a}{2}\frac{\rho(1+\sin(\frac{\pi}{2}-\beta-\alpha))}{|vp|}|vp_i|}{2\rho} \\
&= \frac{\frac{a}{2}(1+\sin(\frac{\pi}{2}-\beta-\alpha))}{2} = \frac{\frac{a}{2}(1+\cos\beta\cos\alpha-\sin\beta\sin\alpha)}{2} \\
&\Leftrightarrow \sin\beta + \frac{\frac{a}{2}\sin\beta\sin\alpha}{2} = \frac{\frac{a}{2}(1+\cos\beta\cos\alpha)}{2} \\
&\Leftrightarrow \sin\beta\left(\frac{2+\frac{a}{2}\sin\alpha}{2}\right) = \frac{\frac{a}{2}(1+\cos\beta\cos\alpha)}{2} \\
&\Leftrightarrow \sin\beta = \frac{\frac{a}{2}(1+\cos\beta\cos\alpha)}{2+\frac{a}{2}\sin\alpha} \\
&\Leftrightarrow \tan\frac{\beta}{2} = \frac{2\sqrt{\frac{a}{2}\sin\alpha+1}-\frac{a}{2}\sin\alpha-2}{\frac{a}{2}(\cos\alpha-1)} \\
&= \frac{2\sqrt{2}\sqrt{a\sin\alpha+2}-a\sin\alpha-4}{a(\cos\alpha-1)}.
\end{aligned}$$

Now, suppose that $p = p_{i+1}$. Then, following an analogous reasoning as before, and using the fact that $|vp_i| < |vp'|$ for triangle $\triangle qp'p_{i+1}$, we get that

$$\begin{aligned}
\sin\beta &= \frac{\frac{|p_ip_{i+1}|}{2}}{2\rho} = \frac{\frac{a}{2}\frac{\rho(1+\sin(\frac{\pi}{2}-\beta-\alpha))}{|vp|}|vp_i|}{2\rho} \\
&< \frac{\frac{a}{2}(1+\sin(\frac{\pi}{2}-\beta-\alpha))}{2} \\
&\Leftrightarrow \tan\frac{\beta}{2} < \frac{2\sqrt{2}\sqrt{a\sin\alpha+2}-a\sin\alpha-4}{a(\cos\alpha-1)}.
\end{aligned}$$

From the results above, we get that β is maximized when $p = p_i$, hence equation (2) is proved.

Finally, we prove equation (3). Let θ, θ_1, and θ_2 be the angles of the triangle px_1x_2 at p, x_1, and x_2, respectively, see Figure 3.

Since $\theta_1 + \theta_2 + \theta = \pi$, we known that

$$\begin{aligned}
|x_1p| + |px_2| &\leq \left(1 + \frac{2\sin\frac{\theta_1}{2}\sin\frac{\theta_2}{2}}{\sin\frac{\theta}{2}}\right)|x_1x_2| \\
&= \left(1 + \frac{2\tan\frac{\theta_1}{2}\tan\frac{\theta_2}{2}}{1-\tan\frac{\theta_1}{2}\tan\frac{\theta_2}{2}}\right)|x_1x_2|.
\end{aligned}$$

Hence, using equation (2) for θ_1 and θ_2, we get the desired formula. □

The results in Lemma 2 depend on the value of a function $a(\varepsilon)$. In order to improve the results in [5] for equilateral meshes, we need to give a value for this function.

2.1 Fixing the number of Steiner points

We first fix the distance between consecutive Steiner points, which implies fixing the total number of Steiner points in each triangular face. In this way, we are improving the upper bound on the distance from x_1 to x_2 through a Steiner point p. In [5], the distance between Steiner points on a segment was defined as $|p_{i-1}p_i| = \sqrt{\frac{\varepsilon}{2}}\sin\frac{\beta}{2}|vp_{i-1}|$, where $\beta = 2\alpha$. So, if we substitute $a(\varepsilon) = \sqrt{\frac{\varepsilon}{2}}$ in equation (2), we get that:

$$\begin{aligned}
\tan\frac{\theta_1}{2} &\leq \frac{2\sqrt{2}\sqrt{\sqrt{\frac{\varepsilon}{2}}\sin\alpha+2}-\sqrt{\frac{\varepsilon}{2}}\sin\alpha-4}{\sqrt{\frac{\varepsilon}{2}}(\cos\alpha-1)} \\
\tan\frac{\theta_2}{2} &\leq \frac{2\sqrt{2}\sqrt{\sqrt{\frac{\varepsilon}{2}}\sin(\frac{\pi}{3}-\alpha)+2}-\sqrt{\frac{\varepsilon}{2}}\sin(\frac{\pi}{3}-\alpha)-4}{\sqrt{\frac{\varepsilon}{2}}(\cos(\frac{\pi}{3}-\alpha)-1)},
\end{aligned}$$

where θ_1, and θ_2 are the angles of the triangle $\triangle px_1x_2$ at x_1, and x_2, respectively, see Figure 3.

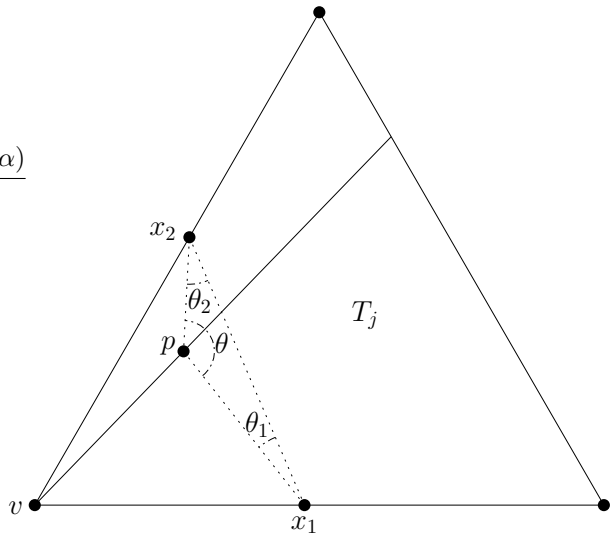

Figure 3: Illustration of Lemma 2.

We want to minimize the upper bound on equation (3) when $a(\varepsilon) = \sqrt{\frac{\varepsilon}{2}}$. Thus, we get that this value is maximized when $\alpha = \frac{\pi}{6}$, i.e., when the Steiner points are placed at the bisectors of the triangles, and minimized when $\alpha = \frac{\pi}{3}$, i.e., when the Steiner points are placed on the sides of the triangles. Hence, using Lemma 2 when placing the Steiner points on the sides of the triangles gives us the following result:

Proposition 3 *Let x_1 and x_2 be two points on two edges e_1 and e_2 of a triangle T_j, and outside the vertex vicinity of the vertex v incident to e_1 and e_2. If p is the Steiner point closest to the intersection between segment x_1x_2 and the segment $\ell_v(j, \frac{\pi}{3})$, then*

$$\begin{aligned}
|x_1p| + |px_2| &= \left(\frac{4\sqrt{2}\sqrt{\sqrt{6\varepsilon}+8}-\sqrt{6\varepsilon}-24}{-4\sqrt{2}\sqrt{\sqrt{6\varepsilon}+8}+\sqrt{6\varepsilon}+8}\right)|x_1x_2| \\
&\lessapprox 1.042\cdot|x_1x_2| \qquad (4)
\end{aligned}$$

Once we have the approximation factor in each of the cells, we need to calculate the approximation factor of

the whole path. We first define a graph G_ε that consists of a set of vertices V_ε, and a set of edges E_ε. Using the corners of the triangles and the set of Steiner points introduced in Definition 1, we create the set of vertices V_ε. For the set of edges we need the notion of neighbor bisectors introduced by Aleksandrov et al. [5]. A bisector is a neighbor to itself. Two different bisectors are neighbors if they belong to the same face of $\mathcal{T}$. Now, consider a pair (ℓ_1, ℓ_2) of neighbor bisectors. We join any pair of nodes p and q lying on ℓ_1 and ℓ_2, respectively. The set of all pairs (p, q) is the set E_ε of edges. Once we have the graph G_ε associated to the discretization, we proceed to compare the weighted length of the approximation path and the actual shortest path in Theorem 4.

Theorem 4 *Let $\pi(s,t)$ be a weighted shortest path between two different vertices s and t on $\mathcal{T}$. There exists a path $\tilde{\pi}(s,t)$ in G_ε such that $\|\tilde{\pi}(s,t)\| \leq \left(1 + \frac{14(4\sqrt{2}\sqrt{\sqrt{6\varepsilon}+8}-\sqrt{6\varepsilon}-8)-16(7+\varepsilon)}{(-4\sqrt{2}\sqrt{\sqrt{6\varepsilon}+8}+\sqrt{6\varepsilon}+8)(7-\varepsilon)}\right) \cdot \|\pi(s,t)\|$.*

Proof. Let $(s = v_0, v_1, \ldots, v_n = t)$ be the ordered set of vertices of $\mathcal{T}$ such that $\pi(s,t)$ intersects their vertex vicinities. Let $a_i, b_i,\ i \in \{0, \ldots, n\}$, be, respectively, the last and first bending point on $\pi(s,t)$ that is in the vertex vicinity of v_i. Thus, we obtain a sequence of bending points $s = b_0, a_0, b_1, a_1, \ldots, a_{n-1}, b_n, a_n = t$ on $\pi(s,t)$ such that segments of $\pi(s,t)$ between a_i and b_i are not contained in the vertex vicinities.

Consider the subsegment $\pi(a_i, b_{i+1})$, for some $0 \leq i < n$. A subpath $\pi'(v_i, v_{i+1})$ is defined [5] as the path from v_i to v_{i+1} along the sequence of bending points of $\pi(a_i, b_{i+1})$. Using the triangle inequality, the fact that $a_i \in S(v_i)$, $b_{i+1} \in S(v_{i+1})$, and the definition of weighted radius, we get that

$$\begin{aligned}\|\pi'(v_i, v_{i+1})\| &\leq \|v_i a_i\| + \|\pi(a_i, b_{i+1})\| + \|b_{i+1} v_{i+1}\| \\ &\leq \frac{\varepsilon}{7}\omega_{min}(v_i)d(v_i) + \|\pi(a_i, b_{i+1})\| \\ &\quad + \frac{\varepsilon}{7}\omega_{min}(v_{i+1})d(v_{i+1}).\end{aligned}$$

Therefore, we obtain the path $\pi'(s,t) = \pi'(s, v_1) \cup \pi'(v_1, v_2) \cup \ldots \cup \pi'(v_{n-1}, t)$. Let $x_j^i,\ j = 1, \ldots m$, be the inner bending points of the subpath $\pi(a_i = x_0^i, b_{i+1} = x_{m+1}^i)$. For each $j = 0, \ldots, m$, we define the point p_j^i to be the closest Steiner point to the intersection between $[x_j^i, x_{j+1}^i]$ and $\ell_v(j, \frac{\pi}{3})$, where v is the common endpoint of the edges containing x_j^i and x_{j+1}^i. Now, we create the path $\pi''(s,t) = \pi''(s, v_1) \cup \pi''(v_1, v_2) \cup \ldots \cup \pi''(v_{n-1}, t)$, where

$$\pi''(v_i, v_{i+1}) = (v_i, p_0^i, x_1^i, p_1^i, x_2^i, \ldots, x_m^i, p_m^i, v_{i+1}).$$

Let $A = \frac{8\sqrt{2}\sqrt{\sqrt{6\varepsilon}+8}-2\sqrt{6\varepsilon}-32}{-4\sqrt{2}\sqrt{\sqrt{6\varepsilon}+8}+\sqrt{6\varepsilon}+8}$. It follows from (4) that $\|\pi''(v_i, v_{i+1})\| \leq (1+A)\|\pi'(v_i, v_{i+1})\|$. Thus,

$$\begin{aligned}\|\pi''(s,t)\| &= \sum_{i=0}^{n-1}\|\pi''(v_i, v_{i+1})\| \leq (1+A)\sum_{i=0}^{n-1}\|\pi'(v_i, v_{i+1})\| \\ &\leq (1+A)\sum_{i=0}^{n-1}\left(\|\pi(a_i, b_{i+1})\| + \frac{\varepsilon\kappa_i}{7}\right), \qquad (5)\end{aligned}$$

where $\kappa_i = \omega_{min}(v_i)d(v_i) + \omega_{min}(v_{i+1})d(v_{i+1})$, so it remains to determine an upper bound for the sum $\sum_{i=0}^{n-1}\kappa_i$. So, using the definition of $d(\cdot)$ it follows that

$$\begin{aligned}\kappa_i &\leq \|v_i a_i\| + 2\|\pi(a_i, b_{i+1})\| + \|b_{i+1} v_{i+1}\| \\ &\leq 2\|\pi(a_i, b_{i+1})\| + \frac{\varepsilon\kappa_i}{7} \Longrightarrow \kappa_i \leq \frac{14}{7-\varepsilon}\|\pi(a_i, b_{i+1})\|.\end{aligned}$$

This, when substituted in equation (5) implies that

$$\begin{aligned}&(1+A)\sum_{i=0}^{n-1}\left(\|\pi(a_i, b_{i+1})\| + \frac{\varepsilon\kappa_i}{7}\right) \\ &\leq (1+A)\sum_{i=0}^{n-1}\left(\|\pi(a_i, b_{i+1})\| + \frac{\varepsilon}{7}\cdot\frac{14}{7-\varepsilon}\|\pi(a_i, b_{i+1})\|\right) \\ &= (1+A)\frac{7+\varepsilon}{7-\varepsilon}\sum_{i=0}^{n-1}\|\pi(a_i, b_{i+1})\| \leq (1+A)\frac{7+\varepsilon}{7-\varepsilon}\|\pi(s,t)\|. \qquad (6)\end{aligned}$$

Finally, two consecutive Steiner points p_j^i and p_{j+1}^i lie on neighbor sides, and v_i belongs to the same edge as p_0^i and v_{i+1} belongs to the same edge as p_m^i. Therefore, the sequence of points $(v_i = p_0^i, p_1^i, \ldots, p_m^i = v_{i+1})$ defines a path $\tilde{\pi}(v_i, v_{i+1})$, such that $\|\tilde{\pi}(v_i, v_{i+1})\| \leq \|\pi''(v_i, v_{i+1})\|$. If we combine all the paths $\tilde{\pi}(s, v_1), \ldots, \tilde{\pi}(v_{n-1}, t)$, we get that $\|\tilde{\pi}(s,t)\| \leq \|\pi''(s,t)\| \leq (1+A)\frac{7+\varepsilon}{7-\varepsilon}\|\pi(s,t)\|$. And the result is proved. □

2.2 Fixing the approximation factor of segment joining two points

The other parameter that we can fix is the approximation factor in each of the triangular cells. By doing this, we are optimizing the number of Steiner points placed in the faces. Using the approximation factor given by Aleksandrov et al. [5], we prove that the distance between consecutive Steiner points can be decreased, see Lemma 5. Due to space limitations, we defer the proof to the full version of the paper.

Lemma 5 *Let e_1, e_2 be two edges adjacent to v in T_i, and let x_1, x_2 be two points in e_1 and e_2, respectively. Let $|p_{i-1}p_i| = \frac{4(\varepsilon+2\sqrt{\varepsilon}\sqrt{\varepsilon+4})}{\sqrt{3}(\varepsilon+4)}\sin\frac{\pi}{3}|vp_{i-1}|,\ i \in \{1, \ldots, k\}$, be the distance between two consecutive Steiner points in side e_2. Let p be the closest Steiner point to x_2, then*

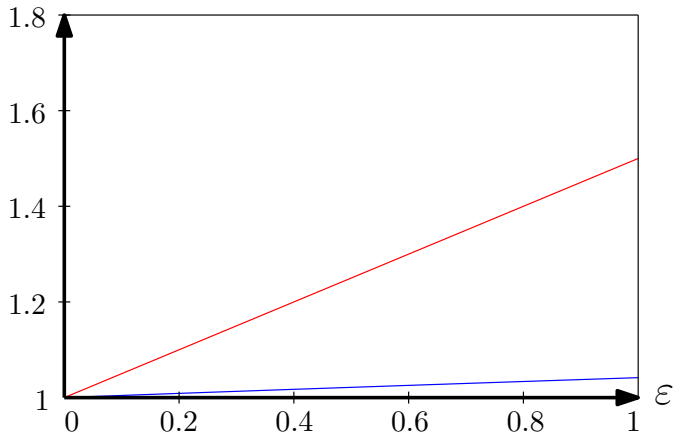

Figure 4: Comparison of approximation factor on a cell. The red function represents $y = 1 + \frac{\varepsilon}{2}$ from [5], and the blue function represents $y = \left(\frac{4\sqrt{2}\sqrt{\sqrt{6\varepsilon+8}}-\sqrt{6\varepsilon}-24}{-4\sqrt{2}\sqrt{\sqrt{6\varepsilon+8}}+\sqrt{6\varepsilon}+8}\right)$ from Proposition 3.

$$|x_1 p| + |p x_2| \leq \left(1 + \frac{\varepsilon}{2}\right) |x_1 x_2|.$$

The next lemma gives us an estimation on the number of Steiner points inserted on a particular side of a triangle and on their total number. The result is obtained by using Lemma 5, and the proof can be found in the full version of the paper.

Lemma 6 *1. The number of Steiner points inserted on a side of a triangle T_i is upper bounded by* $\frac{\log_2 \frac{2|\ell|}{r(v)}}{\log_2 e} \frac{3(\varepsilon+4)^3}{(2\varepsilon+4\sqrt{\varepsilon}\sqrt{\varepsilon+4})(20\varepsilon^2+76\varepsilon-(2\varepsilon+24)\sqrt{\varepsilon}\sqrt{\varepsilon+4}+48)} \log_2 \frac{2}{\varepsilon}$.

2. The total number of Steiner points on $\mathcal{T}$ is less than $C(\mathcal{T}) \frac{9n(\varepsilon+4)^3}{(2\varepsilon+4\sqrt{\varepsilon}\sqrt{\varepsilon+4})(20\varepsilon^2+76\varepsilon-(2\varepsilon+24)\sqrt{\varepsilon}\sqrt{\varepsilon+4}+48)} \log_2 \frac{2}{\varepsilon}$, *where* $C(\mathcal{T}) = \frac{\log_2 \frac{2|\ell|}{\min_{v \in \mathcal{T} r(v)}}}{\log_2 e}$

3 Discussion and future work

We provide some figures where we compare our results with the ones given by Aleksandrov et al. [5]. First, Figure 4 shows the error we commit when the segment between two points on the boundary of two adjacent edges of the tessellation is approximated by the subpath through a Steiner point. The red function represents the error obtained in [5], while the blue function represents the error obtained in Proposition 3, for values of ε in $[0, 1]$. Looking at Table 2, we notice that the error committed by our approach in each cell is about 70% less than using results in [5].

Secondly, in Figure 5 we depict the error obtained when the actual shortest path is approximated by the approach in [5] (see red function) and our result in Theorem 4 (see blue function). The error is shown for values of ε in the interval $[0, 1]$. These two functions show that our result is at least $\frac{5(1+\varepsilon)(7-\varepsilon)}{7(5+\varepsilon)}$ times better than the one provided in [5], i.e., about 150%. See also Table 3 for certain values of ε.

Recall that, in Figures 4 and 5, the approximation factors are obtained by using the same number of Steiner points in our result and in [5].

Finally, let p_i, p_{i+1} be two consecutive Steiner points on a segment from a vertex v on a triangular cell inclined by α radians. Then, Figure 6 represents the distance between p_i and p_{i+1}, divided by the distance $|vp_i|$. The function in red shows the results from [5] when placing the points on the bisector from v, while the function in blue shows our results when placing the points at the

ε	$1 + \frac{\varepsilon}{2}$	$\frac{4\sqrt{2}\sqrt{\sqrt{6\varepsilon+8}}-\sqrt{6\varepsilon}-24}{-4\sqrt{2}\sqrt{\sqrt{6\varepsilon+8}}+\sqrt{6\varepsilon}+8}$
0	1	1
0.1	1.05	1.0044
0.2	1.1	1.0088
0.4	1.2	1.017
0.6	1.3	1.025
0.8	1.4	1.033
0.9	1.45	1.037
1	1.5	1.041

Table 2: Comparison of approximation factor on a cell.

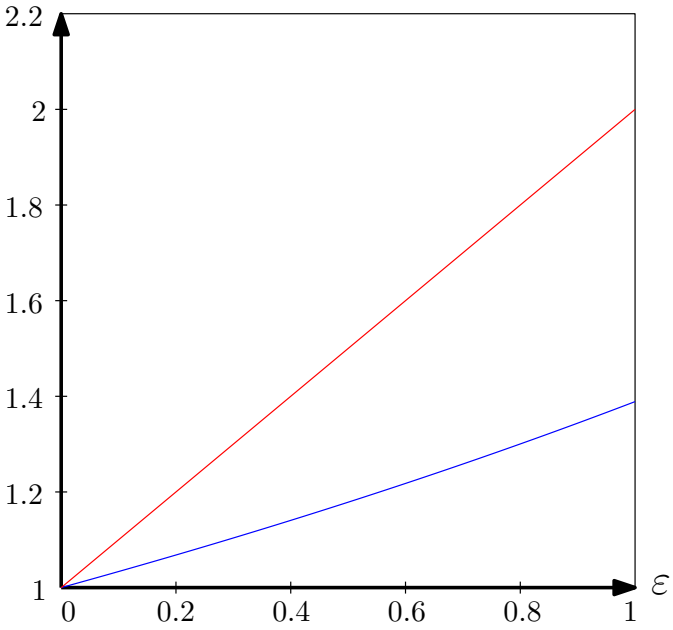

Figure 5: Comparison of approximation factor of paths. The red function represents $y = 1 + \varepsilon$ from [5], and the blue function represents $y = \left(1 + \frac{14(4\sqrt{2}\sqrt{\sqrt{6\varepsilon+8}}-\sqrt{6\varepsilon}-8)-16(7+\varepsilon)}{(-4\sqrt{2}\sqrt{\sqrt{6\varepsilon+8}}+\sqrt{6\varepsilon}+8)(7-\varepsilon)}\right)$ from Theorem 4.

ε	$1+\varepsilon$	$1+\frac{14(4\sqrt{2}\sqrt{\sqrt{6\varepsilon}+8}-\sqrt{6\varepsilon}-8)-16(7+\varepsilon)}{(-4\sqrt{2}\sqrt{\sqrt{6\varepsilon}+8}+\sqrt{6\varepsilon}+8)(7-\varepsilon)}$
0	1	1
0.1	1.1	1.033
0.2	1.2	1.068
0.4	1.4	1.14
0.6	1.6	1.217
0.8	1.8	1.3
0.9	1.9	1.343
1	2	1.3889

Table 3: Comparison of approximation factor of paths.

ε	$\frac{1}{2}\sqrt{\frac{\varepsilon}{2}}$	$\frac{2(\varepsilon+2\sqrt{\varepsilon}\sqrt{\varepsilon+4})}{\varepsilon+4}$
0	0	0
0.1	0.111	0.673
0.2	0.158	0.968
0.4	0.223	1.387
0.6	0.273	1.705
0.8	0.316	1.966
0.9	0.335	2.081
1	0.353	2.188

Table 4: Comparison of distance between consecutive Steiner points on the same cell.

sides of the cells. This value, using our result, is about $\frac{7-\sqrt{\varepsilon}}{40}$ times larger than the value given by Lemma 5, which is an improvement of the bound of about 500%. See also Table 4 for some values of $\varepsilon \in [0,1]$. For this result, we are using the same approximation factor for the segment between two bending points of the shortest path on the boundary of the same cell as in [5]. Moreover, another consequence of Lemma 5 is that the number of Steiner points that we add on each cell is less than in [5], see also Lemma 6, part 1. Hence, we decrease the total number of points that are added to the triangulation, see Lemma 6, part 2. Compared to [5], our method reduces the number of Steiner points in at least 4.5 times. Therefore, the space and time complexity of algorithms that compute weighted shortest paths (e.g., Dijkstra's algorithm) using our approach is less than the complexity of these algorithms using previous results.

As future work, it would be interesting to work with other types of regular grids, e.g., square or hexagonal, or take into account other realistic scenarios like triangulated irregular networks. Another possible extension would be to work with 3D environments.

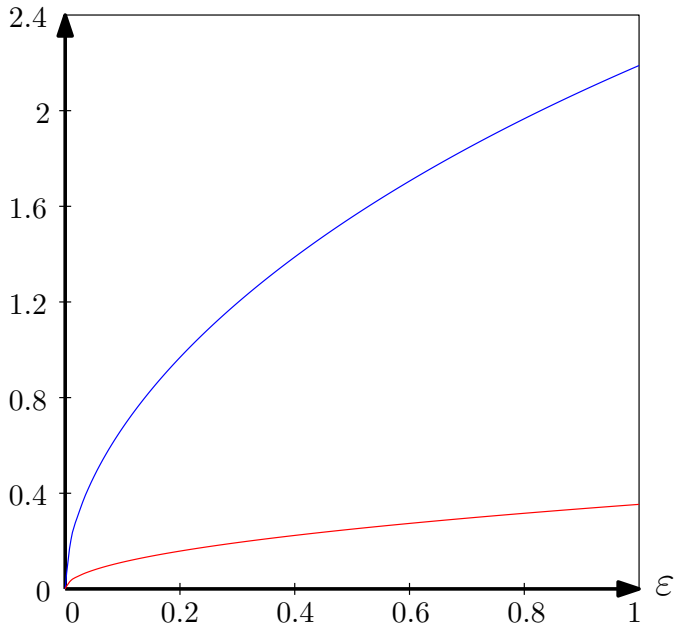

Figure 6: Comparison from Lemma 5. The red function represents $y = \frac{1}{2}\sqrt{\frac{\varepsilon}{2}}$ from [5], and the blue function represents $y = \frac{2(\varepsilon+2\sqrt{\varepsilon}\sqrt{\varepsilon+4})}{\varepsilon+4}$ from Lemma 5.

References

[1] M. Abdalla and B. Nagy. Dilation and erosion on the triangular tessellation: an independent approach. *IEEE Access*, 6:23108–23119, 2018.

[2] Advanced Spaceborne Thermal Emission and Reflection Radiometer Global Digital Elevation Model. Hadoop. `https://asterweb.jpl.nasa.gov`, 2019-08-05. V3.

[3] L. Aleksandrov, M. Lanthier, A. Maheshwari, and J.-R. Sack. An ε-approximation algorithm for weighted shortest paths on polyhedral surfaces. In *Scandinavian Workshop on Algorithm Theory*, pages 11–22. Springer, 1998.

[4] L. Aleksandrov, A. Maheshwari, and J.-R. Sack. Approximation algorithms for geometric shortest path problems. In *Proceedings of the thirty-second annual ACM symposium on Theory of computing*, pages 286–295, 2000.

[5] L. Aleksandrov, A. Maheshwari, and J.-R. Sack. Determining approximate shortest paths on weighted polyhedral surfaces. *Journal of the ACM (JACM)*, 52(1):25–53, 2005.

[6] J.-L. De Carufel, C. Grimm, A. Maheshwari, M. Owen, and M. Smid. A note on the unsolvability of the weighted region shortest path problem. *Computational Geometry*, 47(7):724–727, 2014.

[7] L. de Floriani, P. Magillo, and E. Puppo. Applications of computational geometry to geographic information systems. *Handbook of computational geometry*, 7:333–388, 2000.

[8] Firaxis Games. Civilization V. `http://civilization.com/civilization-5/`. Accessed: 2022-04-14.

[9] P. Kardos and K. Palágyi. Topology preservation on the triangular grid. *Annals of Mathematics and Artificial Intelligence*, 75(1):53–68, 2015.

[10] M. v. Kreveld. Algorithms for triangulated terrains. In *International Conference on Current Trends in Theory and Practice of Computer Science*, pages 19–36. Springer, 1997.

[11] V. Kvachev. Colossal Citadels. `http://colossalcitadels.com`. Accessed: 2022-04-05.

[12] J. S. B. Mitchell. Shortest paths and networks. In J. E. Goodman, J. O'Rourke, and C. D. Toth, editors, *Handbook of Discrete and Computational Geometry, Second Edition*, pages 811–848. Chapman and Hall/CRC, 2017.

[13] J. S. B. Mitchell and C. H. Papadimitriou. The weighted region problem: finding shortest paths through a weighted planar subdivision. *Journal of the ACM (JACM)*, 38(1):18–73, 1991.

[14] B. Nagy and T. Lukić. Dense projection tomography on the triangular tiling. *Fundamenta Informaticae*, 145(2):125–141, 2016.

[15] B. Nagy and E. V. Moisi. Memetic algorithms for reconstruction of binary images on triangular grids with 3 and 6 projections. *Applied Soft Computing*, 52:549–565, 2017.

[16] M. Sharir and S. Sifrony. Coordinated motion planning for two independent robots. *Annals of Mathematics and Artificial Intelligence*, 3(1):107–130, 1991.

[17] N. Sturtevant. A sparse grid representation for dynamic three-dimensional worlds. In *Proceedings of the AAAI Conference on Artificial Intelligence and Interactive Digital Entertainment*, volume 6, 2011.

[18] Z. Sun and J. Reif. Bushwhack: An approximation algorithm for minimal paths through pseudo-euclidean spaces. In *International Symposium on Algorithms and Computation*, pages 160–171. Springer, 2001.